HAL
open science

Mirrors of dynamic curvature for linear solar concentrators

Gang Xiao

▶ To cite this version:

Gang Xiao. Mirrors of dynamic curvature for linear solar concentrators. 2012. hal-00675220

HAL Id: hal-00675220
https://hal.science/hal-00675220

Preprint submitted on 29 Feb 2012

HAL is a multi-disciplinary open access archive for the deposit and dissemination of scientific research documents, whether they are published or not. The documents may come from teaching and research institutions in France or abroad, or from public or private research centers.

L'archive ouverte pluridisciplinaire **HAL**, est destinée au dépôt et à la diffusion de documents scientifiques de niveau recherche, publiés ou non, émanant des établissements d'enseignement et de recherche français ou étrangers, des laboratoires publics ou privés.

Mirrors of dynamic curvature for linear solar concentrators

Gang Xiao (University of Nice, France)

February 29, 2012

Abstract

The linear Fresnel reflector solar technology suffers from the lack of optical precision, due to the dynamic change of optical distance brought about by the rotation of the mirror strips.

We propose a simple method to produce mirror strips with dynamic curvature of high precision, which can be used to significantly enhance the optical concentration efficiency of linear Fresnel reflector solar concentrators. The basic idea is to create a dynamically modifiable depression behind the mirror, that curves the mirror through the elastic deflection of the mirror's substrate.

Introduction

The linear Fresnel reflector (LFR) solar concentrator is one of the most promising solar thermal technologies. It uses multiple independently rotating mirror strips to reflect the Sun's radiations onto a linear receiver at fixed position.

One of the biggest problems of the linear Fresnel technology is the lack of optical precision. Originally, the mirror strips are flat. But flat mirrors offer very limited concentrating capacity, as it is clear that the focus width will not be smaller than the width of the mirror strips. Recently, concave mirror strips with static curvature are proposed, based on the elastic deflection of the glass sheet [7].

Although the statically curved mirrors are more precise than the flat ones and offer a higher concentrating capacity, their optical properties are still less than optimal. As is shown in Figures 4 and 6 of [3], the focus, hence the optical precision, of the mirrors varies with the angle of the Sun. In Section 1, we carry a geometric study of the situation, finding out that for an optimized receiver, the variation of the focal length results in a non-negligeable intercept loss plus an increase in the thermal loss by the receiver.

The limited concentration ratio, hence the large size of the receiver and the high thermal losses from it, is not the only drawback of the variation of the focus. Most LFR receivers now use a multiple of parallel pipes as heat absorber. The variation of the focus leads to a wide variation of the distribution of light

intensity on the different absorbing pipes, creating serious difficulties for the balance of flux and temperature of the fluid within the different pipes.

The only solution to this problem is to use concave mirrors with dynamic curvature. A proposition to this end can be found in [2], but the computations there are rather rough. In fact, the most important point here is that the distribution of the curvature must be as uniform as possible on the whole surface of the mirror, within a wide range of the average curvature.

There are other minor factors to be considered, including the simplicity and the cost of the control mechanism, the resistance to wind load, etc.

The main purpose of this article is to discuss the feasibility of making mirrors of dynamic curvature for LFR concentrators. In Section 2, a simple method to create a uniform curvature variation is proposed. It is shown that using the atmospheric pressure and a reinforcement structure at the back of the mirror, a dynamically variable curvature can be created, with a very high optical precision and a wide range of variation. Moreover, with a small electric fan, a single control point is enough to control the curvature of a mirror strip with more than $10m^2$ of reflective surface.

Detailed calculations are made using concrete examples. The advantage over mirrors of static curvature is obvious. With a higher optical precision, mirrors of dynamic curvature eliminates important intercept loss and reduces the size of the receiver. The gain in performance of the concentrator is estimated to be more than 20%.

Mirrors of dynamic curvature are of special interest for LFR concentrators of small size. Traditionally, a small LFR concentrator must use narrow mirror strips, because a minimal number of mirror strips is required for a reasonable performance. But narrow mirror strips lead to higher cost, due to the multiplication of overhead. Using mirrors of dynamic curvature, concentrators with as few as 4 mirror strips can be constructed, eliminating this problem. A concrete example is described in Section 4.

1 Mirror with static curvature and its focal length

In this section, we present a computation of the optimal aperture width of the receiver for a LFR concentrator using concave mirrors with static curvature. The computed width will later be used to compare with that of mirrors with dynamic curvature.

The focal length of a concave mirror varies with the direction of the focus, as shown by Figure 1. When the mirror moves from position (3) to position (4) due to the rotation of the incoming light (5), the focal point of the reflected light moves from (2) to (7), with a shorter distance towards the mirror. So on the position of the receiver (2), the reflected light scatters out widely.

More precisely, let N be the normal line of the mirror surface at the center p of the mirror, v_1 (resp. v_2) be the vector from the p to the Sun (resp. the center of the receiver), and α be the angle between N and v_2, as shown in Figure 2. Let r be the radius of curvature of the mirror. Then assuming that the width

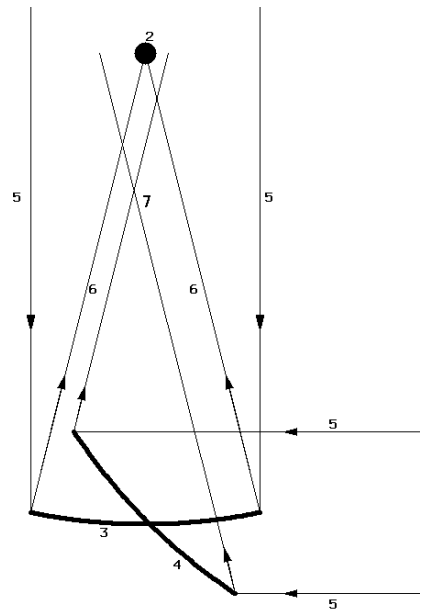

Figure 1: The focal length of a concave mirror

W of the mirror is much smaller than r, the distance δ from p to the focus of the reflected sunlight is given by

$$\delta = \frac{1}{2} r \cos(\alpha) \ .$$

Now if d is the distance from p to the center of the receiver, and if the aperture of the receiver is a plane of width V whose normal line has an angle β with the vector v_2, then the reflected images of light rays coming from the center of the Sun has a width U' given by

$$U' = U'(\alpha, \beta) = \left| \frac{d - \delta}{\delta} \right| W \cos(\alpha) / \cos(\beta) \ .$$

Adding the Sun's angular diameter and enginerring error margins, we get the total width U of the image of the sunlight on the receiver

$$U = U(\alpha, \beta) = \left(\left| \frac{d - \delta}{\delta} \right| W \cos(\alpha) + cd \right) / \cos(\beta) \tag{1}$$

where c is the angular diameter of the cone of the reflected sunlight from p. In practice, engineering error margins other than that resulting from the problem of focal distance can be encorporated into c. As the angular diameter of the Sun is about 0.009 (9 mrad), a typical value of c is 0.015 with 6 mrad for the combined

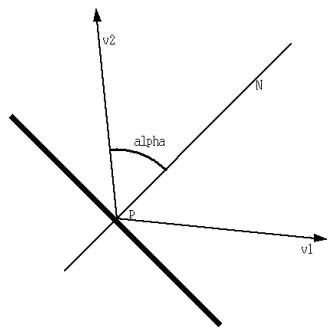

Figure 2: Reflection of a mirror

statistical error margin such as tracking error, surface error, manufacturing error of the components, etc. (see for example [1]).

The proportion of the reflected sunlight that hits the aperture of the receiver is given by

$$\eta = \eta(\alpha, \beta) = \begin{cases} 1 & \text{if } U \leq V \\ V/U & \text{if } U > V \end{cases} \tag{2}$$

This is the intercept efficiency with given angles and given widths.

Now let γ be the angle between the Sun and the zenith. We have $\alpha = \frac{1}{2}(\gamma - \beta)$, or $\gamma = \beta + 2\alpha$. For γ varying within a range $[\gamma_1, \gamma_2]$, the total amount of the radiative energy reflected by the mirror is given by the integral

$$T = T(\beta) = \int_{\gamma_1}^{\gamma_2} F \cos(\alpha)\, d\gamma = \int_{\gamma_1}^{\gamma_2} F \cos\left(\frac{1}{2}(\gamma - \beta)\right) d\gamma \ ,$$

where F is a constant. And by (2), the amount of the reflected radiation that hits the receiver aperture is

$$S = S(V, \beta) = \int_{\gamma_1}^{\gamma_2} F \eta(\alpha, \beta) \cos(\alpha)\, d\gamma \ .$$

Therefore we have the average intercept efficiency of the mirror given by

$$e(V, \beta) = S(V, \beta) / T(\beta) \ , \tag{3}$$

and the average intercept efficiency $E(V)$ of the whole LFR concentrator can be obtained by taking the average of $e(V, \beta)$ over all mirror strips of the concentrator.

This mathematical model can be used to determine the optimal aperture width V of the receiver. To do so, we take as example the configuration of the

concentrator described in [3]. See Table 1 of [3] for the data of the configuration. Note that $W = 0.4m$ for this case, and the height of the receiver is $2.5m = 6.25W$ over the mirror field. There are 5 mirrors at each side of the receiver, with respective values of β at 6.28°, 18.26°, 28.81°, 37.60°, 44.71°.

Suppose that the concentrator is installed with a north-south axis, and we take $\gamma_2 = -\gamma_1 = 65° = 1.1345$, corresponding to a daily movement of the Sun from 7:40 am to 16:20 pm.

The mirror curvature given in Table 1 of [3] is adjusted to $r = 2d$, in other words the focus of the mirror strip is on the receiver when $\alpha = 0$. In this case, if $V = 0.1m = 0.25W$ as suggested in [3, Figure 7], a numerical integration on (3) gives $E(0.25W) = 0.914$, in other words the entercept miss is as high as 8.6%.

The graph of the function $1 - E(V)$ is shown in Figure 3. The optimal value of V/W depends on the thermal loss of the receiver, and can be determined via Figure 3. For example, assume that increasing V/W by 0.01 increases the thermal loss by 0.6% with respect to the amount of energy absorbed by the receiver. Then the optimum of $E(V)$ is obtained at a point of the curve where the slope of the tangent is $dE/d(V/W) = 0.6$. The dotted line in the graph shows that this point is near $V/W = 0.28$, for $1 - E(V) \sim 6.5\%$.

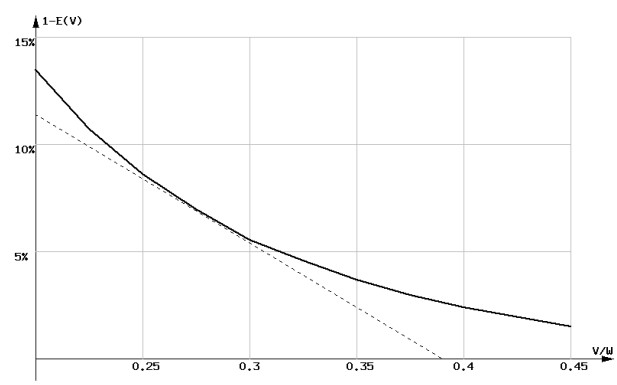

Figure 3: The intercept miss as a function of V/W

Note that the highest values of $e(V, \beta)$ occurs when $|\gamma|$ is near its maximum, and hence the mirror efficiencies are lowest due to the cosine factor. Therefore the variation of the focal lengths of mirrors with static curvature worsens the fluctuation of the output of the LFR concentrator.

2 Mirrors of dynamic curvature

The best material for a solar mirror is the back surface glass mirror, for its performance, durability and low cost. And a concave glass mirror can be formed from a flat glass sheet, via elastic deflection of the glass. For example, [7]

describes a method to form a concave mirror of static curvature using elastic deflection.

Elastic deflection of the glass sheet can also be used to form a concave mirror of dynamic curvature. The difficulties are the simplicity of the control, a sufficient range of the variation of the curvature, and the precision of the distribution of the curvature over the whole surface of the mirror and within the whole range of the variation.

The dynamic elastic deflection can be dynamically created and maintained by the atmospheric pressure, as in Figure 4 that shows a transversal section of the mirror strip. A back structure (12) encloses an essentially hermetic depression chamber (13) behind the glass mirror sheet (11), and a small electric fan or air pump (14) evacuates the air within the depression chamber, creates a slight depression within the chamber. The difference in atmospheric pressure before and behind the glass sheet exercises a uniform normal load (15) on the sheet, resulting in an elastic deflection of it.

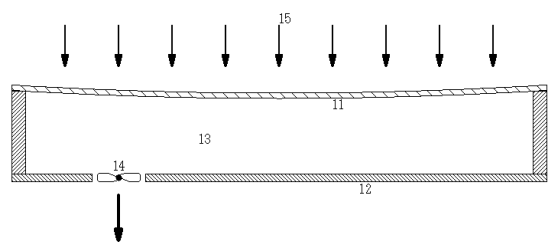

Figure 4: Transversal section of a mirror with its depression chamber

Changing the speed of the fan (or pump) changes the level of the depression, hence the uniform normal load, hence the curvature of the mirror sheet. A sensor can be inserted in the depression chamber, that detects either the level of the depression or the amount of deflection. The output of the sensor can be used as feedback for the control of the fan.

Alternatively, a common depression room can be installed for a multiple of mirror strips, and a more powerful fan, such as that of a vacuum cleaner, is attached to the depression room to create a depression in it. The depression chambers of the multiple of mirror strips are connected to the depression room via hoses. An electrically controled valve is installed in the connection hose between the depression room and the depression chamber of each mirror strip, to control the level of the depression in the latter. Another electric valve links the depression chamber and the environment, so that the depression can be released if it becomes too deep.

The glass mirror sheet is also subject to the gravitation load, which varies with the rotational position of the mirror. As the curvature of the mirror is relatively small, the gravitation is very close to a uniform load on the mirror sheet, so it can be incorporated into the load created by the depression, as long

as it does not generate by itself a deflection exceeding the required amount.

The main point here is that the elastic deflection of a uniform sheet under a uniform normal load is not of constant curvature. According to the Euler-Bernoulli beam equation[9], the bending moment of the glass sheet under the uniform load, at a point p of distance x to the center of the sheet, is

$$M(x) = \frac{F}{2}\left(W^2/4 - x^2\right) \ ,$$

where F is the load per unit length, and W is the width of the mirror sheet as in Section 1.

The curvature of the mirror at the point p is

$$\tau(x) = \frac{M(x)}{EI(x)} = \frac{F\left(W^2/4 - x^2\right)}{2EI(x)} \ , \tag{4}$$

where E is the Young's modulus of the material, and $I(x)$ is the second moment of area. If the only resistance to the deflection comes from the glass sheet, then $I(x)$ is a constant, and the curvature is a quadratic function. This is not desirable, as we want the curvature to be as close to a constant function as possible.

This can be done by adding a reinforcement structure to the back of the glass sheet, as shown in Figure 5. The reinforcement structure consists of parallel bars that help resisting to the deflection of the glass sheet.

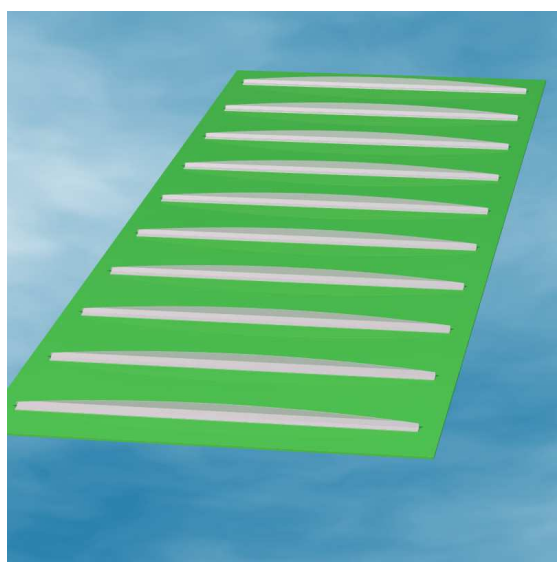

Figure 5: Reinforcement structure at the back of the mirror

Here we assume that the parallel reinforcing bars are not bonded to the back of the mirror, but their ends are pushed against the back of the mirror. Under

this setup, the curvature formula (4) can be re-written as

$$\tau(x) = \frac{F\left(W^2/4 - x^2\right)}{2\left(E_1 I_1 + E_2 I_2(x)\right)}\ , \tag{5}$$

where E_1 and I_1 are the Young's modulus and second moment of the glass sheet, and E_2 and $I_2(x)$ are that of the parallel bars. Now if the parallel bars are constructed in a way such that

$$I_2(x) = \frac{a\left(W^2/4 - x^2\right) - E_1 I_1}{E_2}\ , \tag{6}$$

where a is a constant coefficient, then the curvature $\tau(x) = \frac{F}{2a}$ is constant.

If the reinforcing bars are bonded to the back of the mirror, the second moment of area is higher than in (5), but the principle remains the same.

An example of an angled bar with variable second moment of area is illustrated in Figure 6. For the stability of the bar, the angle is slightly smaller than 90°.

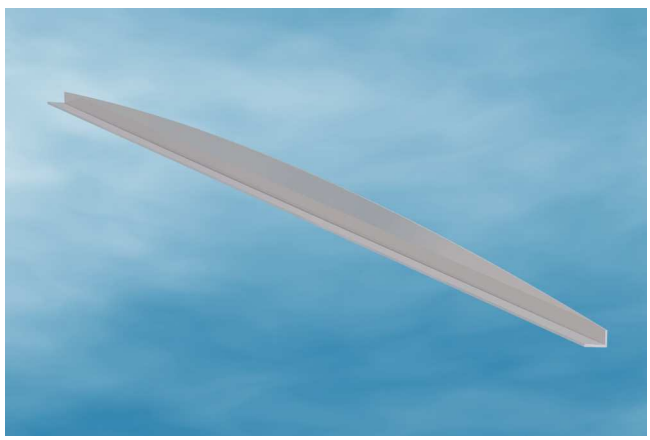

Figure 6: A reinforcing bar with variable second moment of area

Of course, in reality this can never be exactly as in (6), because when $|x|$ is close to $W/2$, the first term of the numerator in (6) is close to 0, hence $I_2(x)$ would be negative, which is impossible to realize.

The solution is to cut the bars to a length shorter than W. Within the length of the bars, the second moment is as given by (6), so that the curvature is theoretically constant; beyond the length of the bars, the curvature, hence the tangent plane, of the mirror sheet is approximative, so that optical aberration occurs. The length of the bars can be chosen so that this approximation is optimal, not only in that the extent of the aberration is minimal, but also in that the area of the mirror surface where aberration occurs is minimal.

More precisely, let L be the length of the bars, and let $R = \frac{E_1 I_1 + E_2 I_2(0)}{E_1 I_1} = \frac{aW^2}{4E_1 I_1}$. The optimal ratio L/W depends only on R, and the higher is R, the

smaller are the aberrations. Note that a higher R also means that the mirror is more rigid, so that its curvature is less sensitive to the random wind load.

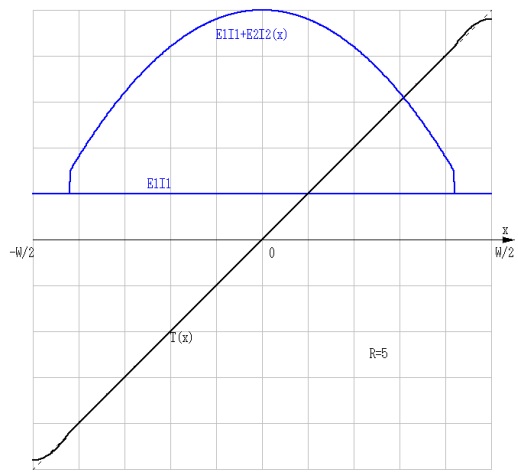

Figure 7: Tangent curve of the mirror for $R = 5$

Figure 7 shows the tangent $T(x)$ of the mirror surface for the case of $R = 5$, and the blue curve in Figure 7 is the curve of second moment of area $E_1 I_1 + E_2 I_2(x)$. Note that it is the tangent of the mirror surface that governs the direction of the reflected light rays, and that for the ideal situation where the curvature is constant everywhere, the tangent curve should be a straight line, as is indicated by the dotted line in the graph.

We have chosen a small value of R for Figure 7, because for higher R the curve $T(x)$ is too close to the straight line for the difference to be graphically visible.

By construction, one sees that the shape of the curve $T(x)$, hence the deviation in the tangent, does not depend on the average curvature. So the optical aberration is a constant proportion of the mirror width W, not depending on the focal distance. And the maximal (average) curvature of the mirror is limited only by the strength of the materials, while the minimal curvature is limited by that introduced by the gravitation load.

We will see from the concrete example in the next section that usually, this range of the variation of the curvature is more than sufficient.

Figure 8 shows the optimal ratio L/W with respect to R. The curve Q is the proportion of the surface of the mirror for which the optical aberration due to the deviation in the tangent is less than $0.005W$.

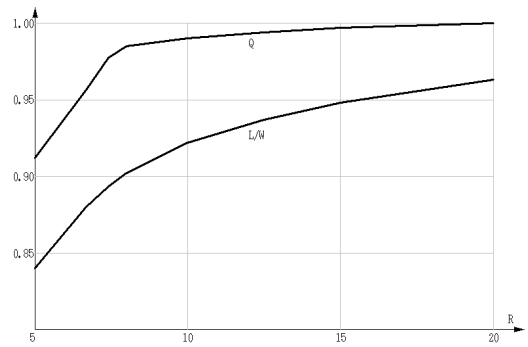

Figure 8: Optimal ratio L/W versus R

3 A concrete example

We can again use the configuration of the concentrator in [3] as an example for a concrete computation of the mirror. However, this configuration is a small one, while concentrators for power generation are usually bigger. As small concentrators will be studied in the next section, here we multiply all the dimensions in [3] by 4. That is, the mirror width is $1.6m$, and the distance between adjacent mirrors is $0.6m$. Moreover, we follow the computations in [12] that recommend a higher receiver, to assume that the receiver is $13m$ above the mirror field (instead of $10m$).

Under this configuration, the maximal curvature occurs for mirror strips near the center of the mirror field, when they are turned perpendicularly towards the receiver. The minimal radius of curvature is $r = 2 \times 13m = 26m$.

Assume that the mirror is made of ordinary glass with a thickness of $5mm$. We have

$$E_1 I_1 = 70GPa \times 5^3 \times 1000mm^4/12 = 730Nm^2$$

per meter of length.

The reinforcing bar at the back of the glass sheet is an L-shaped steel angle, with a thickness of $2mm$, and the width of the leg touching the back of the glass is $15mm$. Its hight is variable according to the requirement of the variable second moment of area, with a maximum of $33mm$ at the center of the bar. At this point, the second moment of area of the bar is

$$E_2 I_2 (0) = 200GPa \times 40^3 \times 2mm^4/12 = 2133Nm^2 \ ,$$

and the maximal distance from the neutral axis to extreme fibers is $e_2 = 20mm$.

In fact, this computation can be easily done by first putting the neutral axis at a point q that is $20mm$ below the top of the bar, then checking that above and below q, the second moments are the same.[8]

At a point of the bar away from the center, both the second moment $E_2 I_2(x)$ and the maximal distance to the extreme fibers are smaller than the corresponding values at the center.

Now assume that parallel reinforcing bars are positioned at a distance of $32.5cm$ from each other. Then for each meter of length, the second moment of area of the bars is $2133Nm^2/0.325 = 6563Nm^2 = 9E_1I_1$, or $R = 10$.

According to Figure 8, the bars extend to a length of $0.92W = 1.47m$.

The level of depression needed to create the curvature can be determined via (5), for the point $x = 0$:

$$26m = r = \frac{1}{\tau(0)} = \frac{14600Nm^2}{0.64Fm^2}m^{-1} = \frac{22810N}{F}m^{-1} ,$$

or $F = 880Nm^{-2} = 9mbar$. As the gravitation amounts to $1.3mbar$, the maximal radius of curvature is $26m \times 9/1.3 = 180m$, which is much more than what is needed (no more than $50m$).

The effect of the wind load on the curvature of the mirror should also be estimated. Wind creates a random load on the mirror surface, changing its curvature. From the above, a deviation of the curvature of 10% corresponds to a pressure of $0.9mbar$, or $9kg/m^2$, which amounts to a wind speed of $42km/h$ if the mirror surface is directly hit. However, LFR mirrors are more horizontally than vertically disposed, and the constant part of the wind pressure can be compensated by varying the depression. Therefore in practice the wind speed of $42km/h$ results in a much lower deviation of the curvature, probably no more than $2-3\%$, which is tolerable.

A higher wind speed will start to affect the optical precision, but a detailed study of the wind load is beyond the scope of this article.

The maximal distance from the mirror to the receiver is $d = \sqrt{13^2 + 9.9^2} = 16.3m$, and the required receiver aperture width is

$$U = cd/\cos(\arctan(9.9/13)) = 0.015 \times 16.3/0.7956 = 0.31m .$$

It remains to be verified that the strength limits of the materials are not exceeded even at the maximal curvature. For the glass sheet, the distance from the extreme fibers to the neutral axis is $e_1 = 5mm/2 = 2.5mm$, hence the maximal strain is

$$70GPa \times e_1/r = 6.7MPa ,$$

which is much less than the usual tensile strength of the glass ($> 30MPa$).

For the reinforcing bar, the maximal strain is $200GPa \times e_2/r = 154MPa$. So choosing a steel grade with yield strength greater than $350MPa$ should be enough.

4 A small LFR concentrator with 4 mirror strips

Small size LFR concentrators are important, because they are more adaptable to various environments than big ones. With mirrors of static curvature, a minimal

number of mirror strips is required, so the biggest problem for reducing the size of the LFR concentrator is the narrowness of the mirrors. Narrow mirrors imply increased overhead of mechanical and structural costs, hence the cost effectiveness is reduced.

With mirrors of dynamic curvature, the number of mirror strips per receiver can be significantly reduced, leading to wider mirrors and hence reduced cost. Here we describe an example to show how this can be done.

The configuration is shown in Figure 9. The mirror width is $W = 1m$, and the receiver height is $3.2m$ above the mirror field. We put a gap of $0.3m$ between adjacent mirror strips, so that the total mirror field width is $4.9m$.

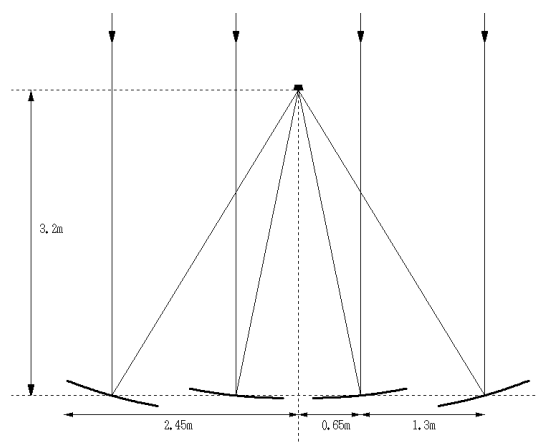

Figure 9: A small LFR concentrator with 4 mirror strips

We use a glass sheet of $3mm$ for the mirror substrate. The minimal radius of curvature is $2\sqrt{3.2^2 + 0.65^2} = 6.5m$. It exercises a maximal curving strain of $70GPa \times 1.5mm/6.5m = 16MPa$, which is acceptable, especially if tempered glass is used. We have

$$E_1 I_1 = 70GPa \times 3^3 \times 1000mm^4/12 = 157.5Nm^2$$

per meter of length.

The reinforcing bar is of thickness $1.5mm$, having a distance of $10mm$ from the extreme fibers to the neutral axis. The second moment of area is $200GPa \times 20^3 \times 1.5mm^4/12 = 200Nm^2$. Placing one bar at each $200mm$ of length, we get $R = 5 \times 200/157.5 + 1 = 7.35$, and the maximal strain on the bar is $200GPa \times 10mm/6500mm = 308MPa$. Therefore, a grade of steel with yield strength $> 600MPa$ is preferred.

As in the preceding section, we find that the maximal depression in the depression chamber is $14mbar$.

The wide mirror leads to an optical aberration when it is not perpendicular to the direction of the receiver, as shown in Figure 10. The reason is that in this case, the different points on the mirror has unequal distance to the receiver, while the curvature is constant. This aberration is inversely proportional to the square of the ratio of mirror-to-receiver-distance versus mirror-width. For a concentrator with 10 or more mirror strips, this aberration is negligeable. But for concentrators with 4 or less mirror strips, this must be taken into account.

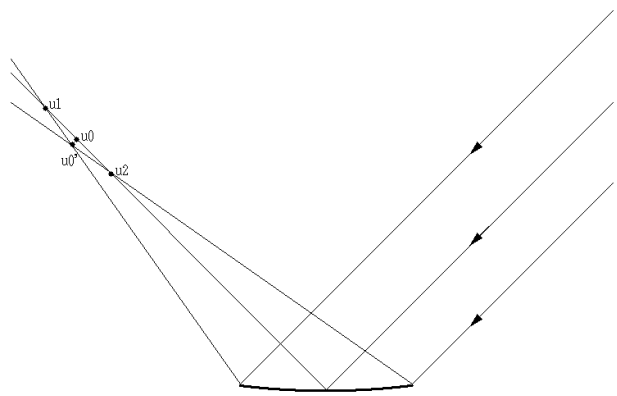

Figure 10: Optical aberration due to unequal distances to the receiver

An easy geometric study shows that the worst case occurs when the normal line of the mirror is at 45° towards the receiver, in which case we have $|u_1 - u_2| \sim 0.53W$, and $|u_0 - u_0'| \sim 0.53W \times \frac{\sqrt{2}}{8} W/d = 0.0937W^2/d$. For our concentrator, the worst case occurs for the two outer mirror strips with $d = \sqrt{3.2^2 + 1.95^2} = 3.75m$, hence $|u_0 - u_0'| \sim 0.025W = 2.5cm$.

Again taking $c = 0.015$ as in (1), and as $\beta = \arctan(2.45/3.2) = 37.4°$, the horizontal aperture width of the receiver should be

$$U = (2.5cm + 0.015 \times 375cm) / \cos(\beta) = 10.2cm \ .$$

With respect to the mirror width of $4m$, the nominal concentration ratio is 39 times. This is slightly better than the concentrator with static mirrors in Section 1, without the important intercept loss.

If secondary reflectors are incorporated in the receiver [12], the emitting absorber width can be reduced to about $7cm$, corresponding to a nominal concentration ratio of 57 times. This is very satisfactory for most applications.

Efforts to further reduce the size of the concentrator and the number of mirror strips per receiver meet with two difficulties. A lower receiver puts more strain to the mirror materials (glass and steel bar), that may exceed their strength limit. And the optical aberration due to unequal distance from points on the mirror to the receiver limits the ratio d/W. Solutions do exist, but these

are beyond the scope of this article. We expect to return to this subject in a later occasion.

5 Comparing with mirrors of static curvature

If we multiply by 4 the size of the example concentrator in Section 1, we get a concentrator with a total mirror width of $16m$ and a receiver height of $10m$. The optimal receiver aperture width becomes $0.28W = 0.45m$.

This can be compared with the example concentrator using mirrors of dynamic curvature in Section 3. We have seen that for this case the aperture width is $0.31m = 0.19W$, with no intercept loss due to the variation of focal length. Note that this width would be slightly smaller if the height of the receiver was not lifted to $13m$.

According to the dotted line in Figure 3, the performance gain of the latter, in intercept loss and thermal loss of the receiver, amounts to 12%.

For the cost comparison, it is difficult to get precise cost information, so we just give some rough estimations.

The mirrors of dynamic curvature reduces the size of the receiver by one third, with a corresponding cost reduction estimated to one fifth. If the cost of the receiver represents 20% of the total cost of the concentrator, the cost reduction amounts to 4% of that of the concentrator.

If we force the LFR concentrator with mirrors of static curvature to use a receiver with the same width $0.19W$ as for the case of dynamic curvature, Figure 3 shows an intercept miss of $C = 15\%$. This is at the same level of the sum of the intercept loss and the cost difference for the optimal case above.

Let G be the total amount of optical energy received by the receiver, H be the thermal loss by the receiver as well as the fluid circuit outside the concentrator. H depends on the operational parameters of the concentrator, but a typical value is $H = 0.15G$.

Now for a concentrator with given size, the value of H does not depend on the type of the mirrors. So the net output of the concentrator is $G - H = 0.85G$ for the case of dynamic curvature, while it is $G - H - C = 0.7G$ for the case of static curvature. And the gain in performance of the former over the latter is $0.85/0.7 - 1 = 21\%$.

On the side of the cost, the main difference between the two methods is with the mirrors. For mirrors with static curvature, the process of forming the precise curvature is a very special one, whose cost is a non-negligeable part of the total cost, even if the curvature is formed using the elasticity of the glass [7], although we lack data for a precise estimation of this cost.

For mirrors with dynamic curvature, first they need the enclosing case at the back to form the depression chamber. But this case replaces the rigidifying structure at the back of the mirror, with comparable cost. The reinforcing bars at the back of the mirror are easy to produce and are of very limited cost.

The sealing of the depression chamber represents a special technical requirement, whose cost is to be compared with the formation of the curvature for

mirrors with static curvature. Our conjecture is that this comparison is favorable for mirrors with dynamic curvature, but this needs confirmation from the industrial side.

An electric fan or air pump is needed to maintain the depression. Most small DC fan having insufficient static pressure specification, an air pump with specifications similar to that used for an aquarium can be selected. For a mirror strip whose surface area exceeds $10m^2$ in general, the cost of the pump and its control circuitry is negligeable. As there is little air flux, the air pump consumes only a few watts and is only turned on when needed, so that its power consumption represents only a fraction of a percentage point of the electricity that the solar concentrator can generate.

For solar concentrators with a size smaller than the above, the mirror of dynamic curvature gives an extra cost advantage due to the fact that the number of mirror strips per receiver can be reduced to 6 or 8 without noticeable drop in performance, against a minimum of 10 or 12 for mirrors with static curvature.

References

[1] Giacomo Barale et al., Optical design of a linear fresnel collector for Sicily, SolarPACES2010

[2] Randolph Brost, Apparatus and method for building linear solar collectors directly from rolls of reflective laminate material, International patent application WO/2010/083292

[3] Jorge Facao and Armando C. Oliveira, Numerical simulation of a trapezoidal cavity receiver for a linear Fresnel solar collector concentrator, Renewable Energy 36 (2011) 90-96

[4] A. Fernández-García et al., Parabolic-trough solar collectors and their applications, Renewable and Sustainable Energy Reviews Volume 14, Issue 7, September 2010, Pages 1695-1721

[5] A. Häberle et al., The Solarmundo line focussing Fresnel collector. Optical and thermal performance and cost calculations. In: International symposium on concentrated solar power and chemical energy technologies, Zürich; 2002.

[6] A. Häberle et al. Linear concentrating fresnel collector for process heat applications. In: Proceedings of the 13th international symposium on concentrated solar power and chemical energy technologies: Seville, Spain; June 20, 2006.

[7] A. Hoermann et al., Method and apparatus of Shaping a Reflector, International patent application WO/2010/111187

[8] W. Pilkey, Analysis and Design of Elastic Beams. John Wiley & Sons 2002

[9] S. Timoshenko, History of strength of materials, McGraw-Hill 1953

[10] F. Trieb et al., Solar electricity generation-a comparative view of technologies, costs and environmental impact, Solar Energy Vol. 59, Nos. l-3, pp. 89-99,1997

[11] G. Xiao, Tilting mirror strips in a linear Fresnel reflector, to appear

[12] G. Xiao, Geometric optimization of a LFR receiver, to appear